Coplanar Waveguide Bandpass Filter—A Ribbon-of-Brick-Wall Design

Fang-Lih Lin, Chien-Wen Chiu, and Ruey-Beei Wu, *Member, IEEE*

Abstract—**This paper proposes a novel ribbon-of-brick-wall design of the coplanar waveguide bandpass filter which is built from cascading several sections of quarter wavelength open-end series stubs. The design originates from modeling the series stub as a system of two asymmetrically coupled transmission lines, which is then made equivalent to a basic filter element of admittance inverter. The relationship between the parameters of the coupled transmission lines and the admittance inverter is derived and the design charts are provided for the convenience of the designers. Systematic procedure is established to design the Chebyshev filter, which is also fabricated and measured. In addition, the quasistatic equivalent lumped circuit models of the discontinuities formed between two sections are evaluated and incorporated into the circuit simulation to get better prediction for the filter performance. The good agreement between simulation results and experimental data justifies the design procedure and validates the present analysis approach.**

I. Introduction

As THE system operating frequency becomes higher and higher, CPW's are increasingly used as transmission lines in MIC and MMIC design. Owing to the uni-planar feature, CPW offers several advantages over its counterpart—microstrip line, such as easy series and shunt connection, no via hole, insensitive to the substrate thickness, and low dispersive effects. In spite of these advantages, applications of CPW, especially for filters, are not so widely as expected because the lack of design data and accurate equivalent circuit model for discontinuities.

In 1976, Houdart [1] proposed the CPW open-end and short-end series stubs and which may be used in the filter design. The two stubs were modeled as a series capacitor and inductor respectively, which are too simple to predict properly the electrical properties. In 1991, Dib *et al.* [2] applied the space-domain full-wallwave integral equation to calculate the scattering parameters of the stubs. From the computation results, they used curve-fitting technique to get the equivalent circuit models. Their models can provide better accuracy but the elements in the models are too complicated to convey reasonable physical meaning. Similarly, Rayit *et al.* [3] used the simulator *em* to calculate the scattering parameters but suggested another equivalent circuit models. Since the circuit model is not enough to realize the filter, they also employed the open-end or short-end shunt stubs. As a result, their filter consumes a large layout area and requires additional air bridges.

Manuscript received August 2, 1994; revised January 19, 1995. This work was supported by the National Science Council, Republic of China, Grant NSC84-2221-E-002-015.

The authors are with the Department of Electrical Engineering, National Taiwan University, Taipei, Taiwan, 10617, Republic of China.

IEEE Log Number 9412045.

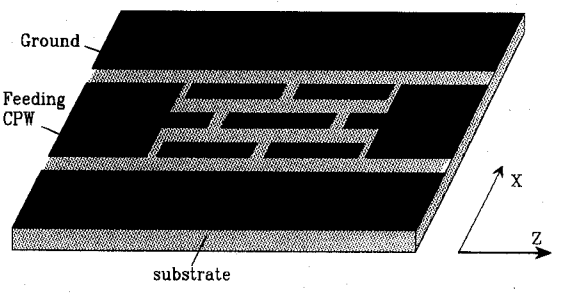

Fig. 1. A ribbon-of-brick-wall CPW bandpass filter.

A few structures were experimentally employed and presented to implement the CPW filter. In 1983, Walliams *et al.* [4] proposed a CPW end-coupled filter using CPW gap or interdigital capacitances as admittance inverters to realize the filter. However, the gap capacitance is usually not large enough for the design of filters, especially wideband bandpass filters. Nguyen [5] suggested the broadside-coupled coplanar waveguide to achieve wide-bandwidth but the main advantages due to the uni-planar feature of CPW will be destroyed. Recently, Chang *et al.* [6] used the CPW shunt inductor as the impedance inverter to realize the band pass filter. The filter occupies larger area due to the shunt stubs and consequently, is not satisfactory in MIC and MMIC which always require high density to reduce the circuit cost.

This paper proposes the design of a novel ribbon-of-brick-wall coplanar waveguide bandpass filter which requires only one metallization plane and is compact in size. The filter is built from cascading several sections of quarter wavelength open-end series stubs. In Section II, a distributed circuit consisting of two asymmetrically coupled CPW's is proposed to model the stub section. By applying the coupled transmission line theory, the stub is made equivalent to an admittance inverter for the filter design in Section III. The effects of the discontinuities formed in the joint of two stub sections are considered in Section IV. They are modeled by lumped capacitances and inductances and are incorporated with the distributed coupled CPW sections to simulate the filter performance. Section V illustrates the design procedure for a Chebyshev type bandpass filter in accordance with the given specifications and presents the measurement results. Finally, some brief conclusions are drawn in Section VI.

II. Coupled Transmission Lines Model for an Open-End Series Stub

Fig. 1 shows the basic layout pattern of the proposed bandpass filter, which looks like a ribbon of brick walls (RBW). The building element of the RBW filter is a quarter-

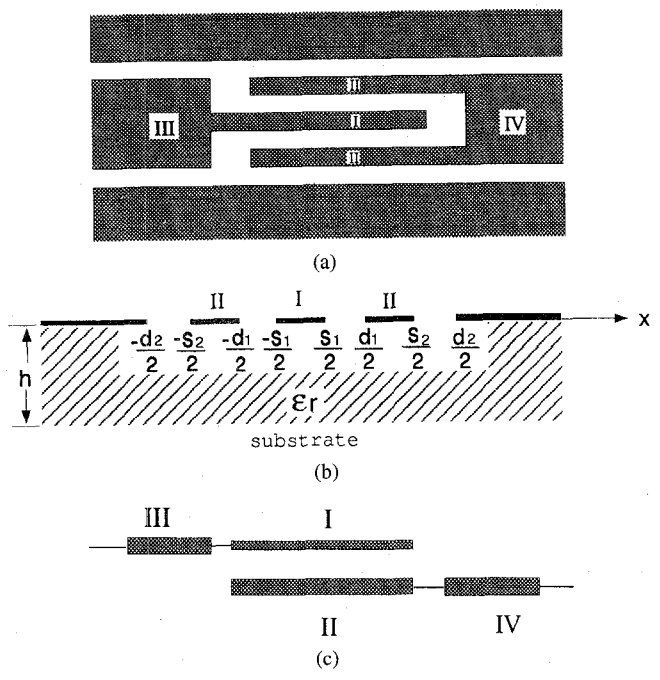

Fig. 2. CPW open-end series stub: (a) layout pattern, (b) cross-section of the coupling region, and (c) equivalent model.

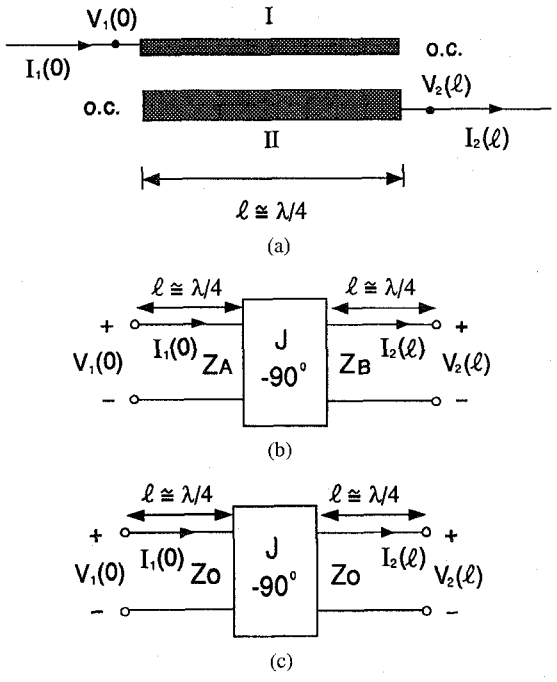

Fig. 3. (a) Asymmetrical coupled transmission lines, (b) admittance inverter, and (c) further approximated equivalent circuit.

wavelength CPW open-end series stub shown in Fig. 2(a). The cross section of the stub element is shown in Fig. 2(b). To begin with, the effects of discontinuities between adjacent stub sections are neglected for simplified analysis. In other words, the connections of lines I and III, II and IV are treated as ideally short, while the gaps between lines II and III, I and IV are treated as ideally open. In light of the mutual coupling between lines I and II, the stub element is modeled as a section of two asymmetrically coupled parallel transmission lines shown in Fig. 2(c).

The coupled transmission lines are made of two coplanar CPW's in parallel. Characterization of the coupled CPW's requires the capacitance and inductance matrices. The variational formulation proposed in [7] is generalized here for the capacitance calculation. Let V_1 and V_2 be the voltages on the strips I and II with respect to the ground conductors. By the circuit theory, the total electric energy per unit length can be expressed as

$$W_e = \tfrac{1}{2}C_{11}V_1^2 + \tfrac{1}{2}C_{12}V_2^2 + C_{12}V_1V_2 \tag{1}$$

where C_{11}, C_{22}, and $C_{12}(<0)$ are the elements in the capacitance matrix $[C]$. On the other hand, it can be obtained by employing the field theory, i.e., [7]

$$W_e = \frac{1}{2}\int_{slot}\int_{slot} G(|x-x'|) \cdot M(x)M(x')\,dx\,dx' \tag{2}$$

where M is the equivalent magnetic current along the slot and G is the associated two-dimensional Green's function of the CPW structure. Note that the equivalent magnetic current should satisfy the constraint that its path integral over a certain slot equals the voltage drop between the two conductors on both sides of the slot.

The constrained variational (2) can be solved to yield the magnetic current distribution subject to imposed voltages V_1 and V_2. The resultant total electric energy gives a realization of the desired capacitances by (1). Choosing three different combinations of the imposed voltages, one can extract the capacitance matrix $[C]$ of the coupled lines. The inductance matrix is then calculated from the capacitance matrix by $[L] = (1/v_0^2)[C_0]^{-1}$ where v_0 is the light velocity in vacuum and $[C_0]$ is the capacitance matrix for the same structure but with the substrate replaced by the free space [8].

Let $\overline{V}(z)$ and $\overline{I}(z)$ denote the vectors of voltages and currents, respectively, along the coupled transmission lines shown in Fig. 3(a). By employing the modal decomposition approach [9], the impedance matrix of the two coupled transmission lines can be derived to be

$$\begin{bmatrix}\overline{V}(0)\\ \overline{V}(l)\end{bmatrix} = \begin{bmatrix}-j[M_V]\overline{\overline{Z}}_o \cot \overline{\overline{k}}l[M_V]^T & j[M_V]\overline{\overline{Z}}_o \csc \overline{\overline{k}}l[M_V]^T\\ -j[M_V]\overline{\overline{Z}}_o \csc \overline{\overline{k}}l[M_V]^T & j[M_V]\overline{\overline{Z}}_o \cot \overline{\overline{k}}l[M_V]^T\end{bmatrix} \cdot \begin{bmatrix}\overline{I}(0)\\ \overline{I}(l)\end{bmatrix} \tag{3}$$

where the diagonal matrices

$$\overline{\overline{k}} = \mathrm{Diag}\{k_i\}; \quad \overline{\overline{Z}}_o = \mathrm{Diag}\{Z_{o,i}\}; \quad i = 1, 2 \tag{4}$$

consist of the propagation constants and characteristic impedances of the two modes, respectively, and the voltage transmission matrix

$$[M_V] = \begin{bmatrix}\phi_{11}, & \phi_{12}\\ \phi_{21}, & \phi_{22}\end{bmatrix} \tag{5}$$

is the eigenmatrix of $[L]\cdot[C]$.

Under the first-order approximation that the two floating ends shown in Fig. 3(a) are ideally open and the propagation constants of two modes are nearly the same, i.e., $I_1(l) = I_2(0) = 0$, $k_1 l \cong k_2 l \cong kl$, then (3) becomes

$$\begin{bmatrix} V_1(0) \\ V_2(l) \end{bmatrix} \cong \begin{bmatrix} -jZ_{11} \cot kl & jZ_{12} \csc kl \\ -jZ_{12} \csc kl & jZ_{22} \cot kl \end{bmatrix} \cdot \begin{bmatrix} I_1(0) \\ I_2(l) \end{bmatrix} \tag{6}$$

where

$$Z_{pq} = Z_{0,1}\phi_{p1}\phi_{q1} + Z_{0,2}\phi_{p2}\phi_{q2} \quad p, q = 1, 2. \tag{7}$$

III. Equivalent Admittance Inverter and Design Charts

The asymmetrically coupled transmission lines with two open ends shown in Fig. 3(a) can be made equivalent to an admittance inverter shown in Fig. 3(b) which is essential in the filter design [10]. The impedance matrix of the inverter circuit can be derived, but with a lengthy expression. In case that $kl \cong \pi/2$, it can be greatly simplified to give

$$\begin{bmatrix} V_1(0) \\ V_2(l) \end{bmatrix} \cong \begin{bmatrix} -jZ_A(J^2 Z_A Z_B + 1) \cot kl & jJZ_A Z_B \\ -jJZ_A Z_B & jZ_B(J^2 Z_A Z_B + 1) \cot kl \end{bmatrix} \cdot \begin{bmatrix} I_1(0) \\ I_2(l) \end{bmatrix}. \tag{8}$$

This can be compared with (6) where $\csc kl \cong 1$ to yield the equivalence relationship

$$\begin{aligned} Z_{12} &= JZ_A Z_B; \\ Z_{11} &= Z_A(J^2 Z_A Z_B + 1); \\ Z_{22} &= Z_B(J^2 Z_A Z_B + 1). \end{aligned} \tag{9}$$

For convenience sake, it is better to use the transmission lines of same characteristic impedance in the filter design. The inverter circuit shown in Fig. 3(b) can be further approximated by the circuit shown in Fig. 3(c) with $Z_o = \sqrt{Z_A \cdot Z_B}$. Then the equivalence between Fig. 3(a) and (c) can be established based on (9). Two parameters are defined for asymmetrically coupled transmission lines and are related to the two parameters of the inverter circuit by

$$\begin{aligned} Z_{avg} &\equiv \sqrt{Z_{11} \cdot Z_{22}} = Z_o(J^2 Z_o^2 + 1) \\ K_{\Delta/2} &\equiv \frac{Z_{12}}{\sqrt{Z_{11} \cdot Z_{22}}} = \frac{JZ_o}{J^2 Z_o^2 + 1}. \end{aligned} \tag{10}$$

Physically, they can be interpreted as the average impedance and coupling coefficient of the coupled transmission lines system, respectively.

It is ready to design the bandpass filter based on the above equivalence relationship. Given the specifications of the bandpass filter, one can determine the parameter $Z_o J$ of each section from the design equations [11], [12] and then the values of $K_{\Delta/2}$ and Z_{avg} from (10). The remaining problem is how to choose efficiently a suitable geometry of the coupled CPW's which can implement the desired values of $K_{\Delta/2}$ and Z_{avg}.

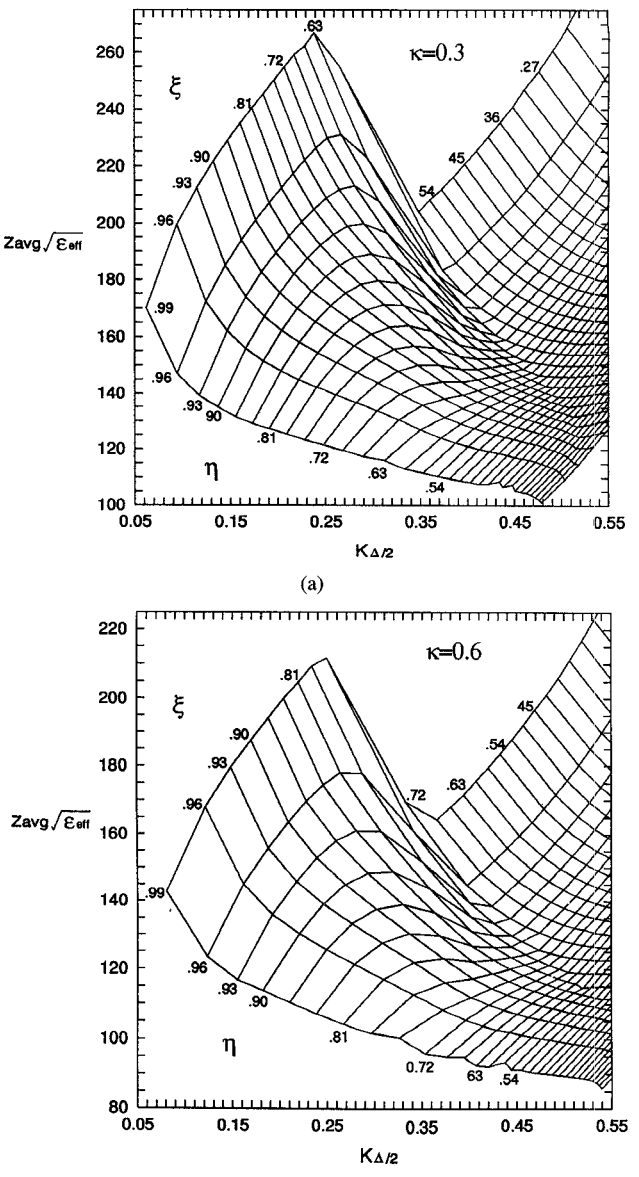

Fig. 4. Design charts for coupled CPW's in the absence of substrate ($\epsilon_r = 1$) with fixed parameter (a) $\kappa = 0.3$ and (b) $\kappa = 0.6$.

Consider the cross section of the coupled CPW's shown in Fig. 2(b). It is advantageous to define three structure parameters by

$$s_1 = \kappa d_1; \quad d_1 = \eta s_2; \quad s_2 = \xi d_2 \tag{11}$$

where $0 < \xi, \kappa, \eta < 1$. Each combination of ξ, κ, η corresponds to a particular structure of coupled CPW's, for which the matrices $[C]$, $[L]$, $[M_V]$, and $\overline{\overline{Z}}_o$ can be calculated to obtain the parameters $K_{\Delta/2}$ and Z_{avg} by (10). Using $K_{\Delta/2}$ and $Z_{avg} \cdot \sqrt{\epsilon_{eff}}$ as the x- and y-axes, respectively, a series of design charts can be constructed by varying the ξ, κ, η values. Fig. 4 shows two examples of design charts for the coupled CPW's with the parameter κ fixed at 0.3 and 0.6, respectively, in the absence of the substrate ($\epsilon_r = 1$). The desired dimension parameters for given $K_{\Delta/2}$ and Z_{avg} can be read from the design charts directly.

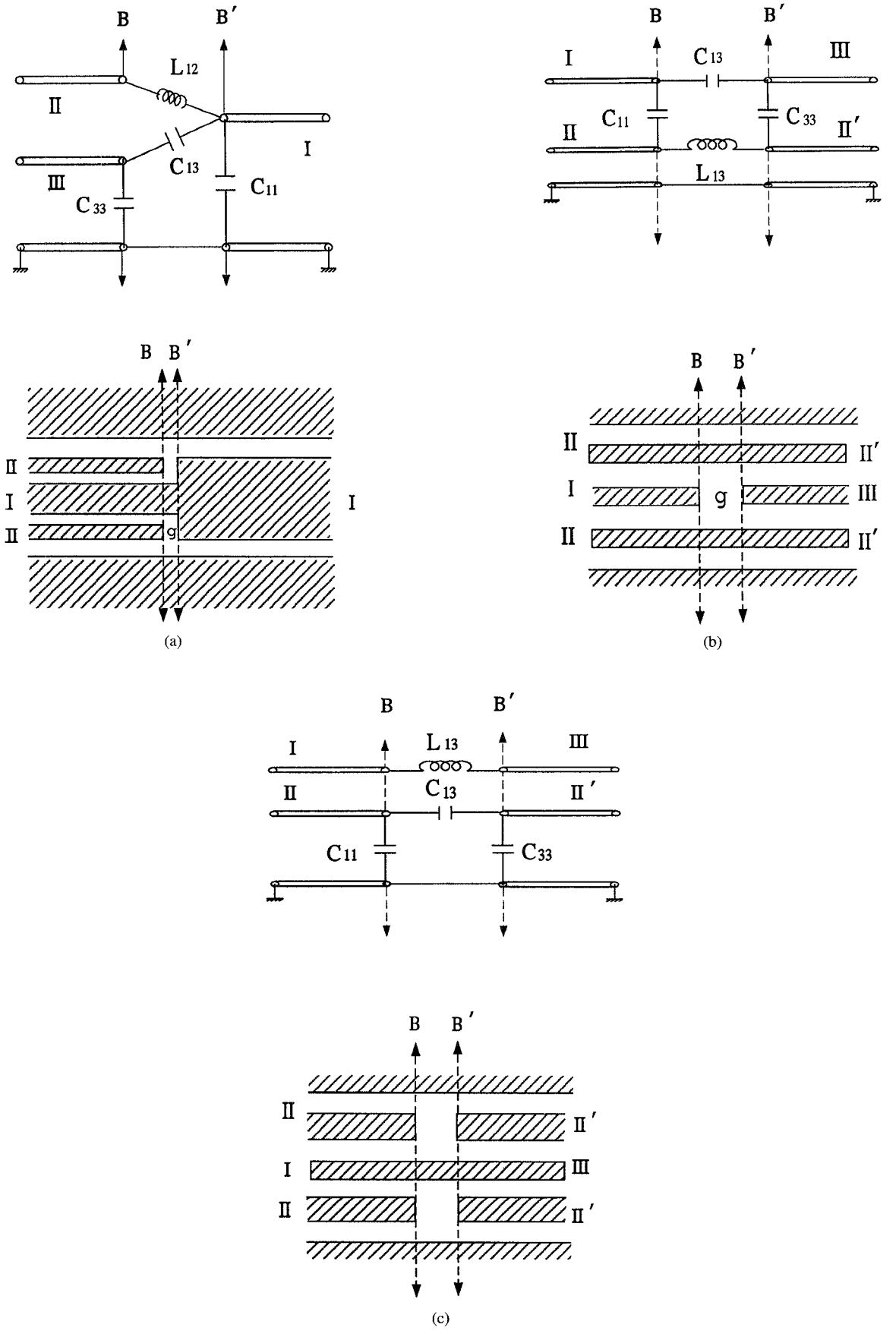

Fig. 5. Discontinuities and their equivalent lumped circuit models at the junctions between (a) stub section and feeding line, (b) the first and second sections, and (c) the second and third sections.

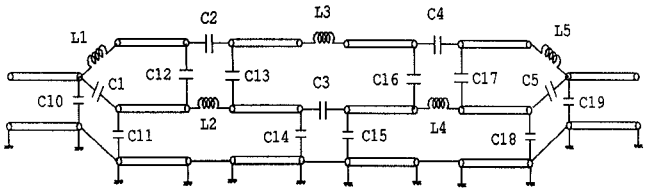

Fig. 6. Equivalent circuit of the whole filter.

In the presence of the substrate, the design charts may differ from those in Fig. 4 by a slight shift. Nonetheless, the substrate-free design charts in Fig. 4 are helpful in locating the desired physical dimensions for a given Z_{avg} and $K_{\Delta/2}$. One can estimate the shift value and incorporate it into the design charts to obtain good approximates of ξ and η.

IV. Analysis and Simulation for Discontinuity Effects

The bandpass filter shown in Fig. 1 is built from cascading several identical sections of open-end series stubs. Discontinuities including the gap and step change are formed at the joints of the sections. They should be modeled properly in order to get better prediction of the filter performance. A closer look of the bandpass filter reveals that the discontinuities fall into three basic categories. With the size much smaller than a wavelength, the discontinuities can be represented in terms of lumped capacitances and inductances under the quasistatic approximation. Fig. 5 shows the three categories of the discontinuities and the corresponding equivalent circuits.

The discontinuity structure shown in Fig. 5(a) happens at the joint of the feeding CPW and the stub section. The gap between the two conductors I and III will cause a substantial charge accumulation near the open end. The resultant electric flux linkages exist partly between the two conductors and partly from the two conductors to the ground conductor, which are modeled by the capacitances C_{13}, C_{11}, and C_{33}, respectively. In addition, there is a step change in width between the two conductors I and II. The redistribution of the current flow near the step change results in additional magnetic flux which can be modeled by a discontinuity inductance. Note that the lumped inductance L_{12} in Fig. 5(a) includes not only the discontinuity inductance but also the transmission line inductance of a small length between the two reference planes B and B′.

Fig. 5(b) shows the discontinuity structure formed at the junction between the first and second, and similarly the third and fourth, sections. The lumped capacitance C_{13} represents the capacitive coupling between the two conductors I and III due to the presence of the gap. The flux linkages flowing from the two conductors to the conductor II-II′ are modeled by the capacitances C_{11} and C_{33}, respectively. Due to the choice of the reference planes, there is a lumped inductance L_{13} for the transmission line in between. Note that the gap capacitances here are approximately calculated by treating all the regions outside the conductor II-II′ as ground. Similar modeling can be employed for the discontinuity structure shown in Fig. 5(c) due to the junction between the second and third stub sections. It is worthy mentioning that the conductors II and II′ have two

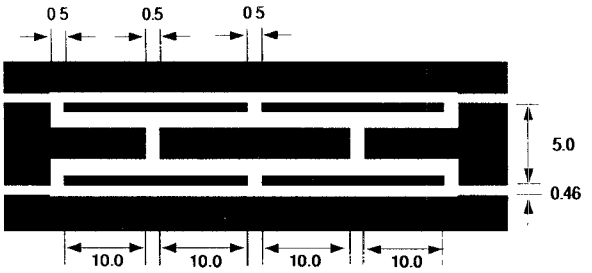

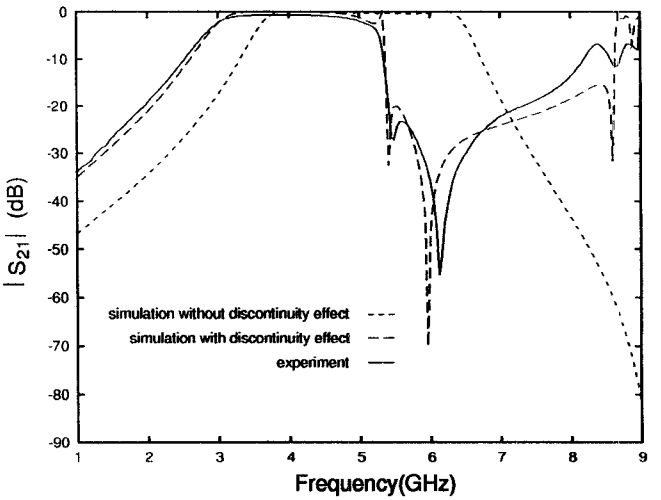

Fig. 7. Simulation results for a periodic RBW filter with and without considering discontinuity effects. Measured data are also included for comparison.

signal strips. Hence, the equivalent capacitances of the two associated gaps should be shunt connected to form the desired lumped capacitances C_{13}, C_{11}, and C_{33} in the equivalent circuit.

Efficient numerical techniques have been established to extract the equivalent capacitances and inductances of the discontinuities. The capacitance calculation is based on the variational formulation proposed in [7], which has been generalized to deal with multiple ports. The inductances are calculated indirectly. A coplanar strip (CPS) structure complementary to the CPW discontinuity is established. Then, the equivalent CPS capacitances are solved and from which the desired CPW inductances can be obtained [13].

The equivalent circuits of the discontinuities shown in Fig. 5 can be incorporated with the coupled transmission lines models of the stub sections shown in Fig. 2(c) to form a complete circuit of the whole bandpass filter. For example, Fig. 6 shows the complete circuit of the four-section bandpass filter shown in Fig. 1. All the circuit elements contain physical meaning such that circuit simulation can be performed to examine the detailed filter response.

Fig. 7 shows the simulation results with and without considering discontinuity effects, which are compared with the experimental data. The filter is fabricated on a substrate with a relative dielectric constant of 4.2 and height of 1.45 mm. The feeding and output CPW's have characteristic impedance of $Z_o = 50\ \Omega$. The measurements are calibrated carefully by the TRL (Thru-Reflect-Line) method [14]. It can be seen that the discontinuity effects will shift the response toward

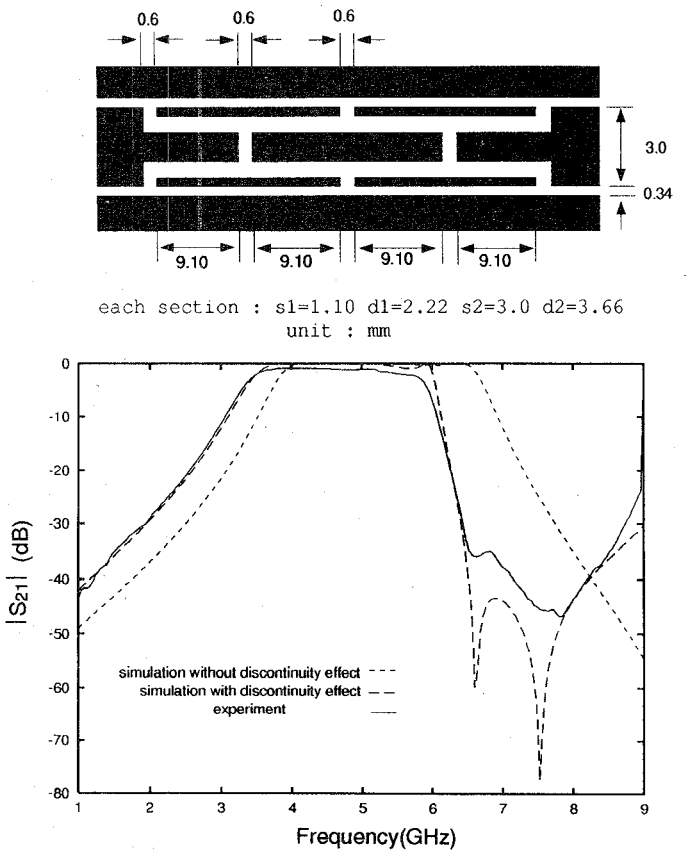

Fig. 8. Simulation results with and without considering discontinuity effects and measured data for a periodic RBW filter with narrower line width.

the lower frequency and distort the behavior at the higher frequency portion. With the discontinuities properly modeled, the simulation results resemble the experimental data and can reasonably account for the irregular behavior of the response at the higher frequency portion. The dips occur near the upper band can be contributed to the additional poles produced by the extra coupling at the gap between resonators [15].

The frequency shift due to the presence of discontinuities can be offset by suitably shortening the section length. Fig. 8 shows the transmission coefficient of a bandpass filter which is similar to that in Fig. 7 but with a shorter section length, a slightly larger gap width, and all other dimensions shrunken by about 60%. The pass band is now roughly centered at 5 GHz after the simple compensation. Due to the choice of narrower lines, the discontinuities have smaller capacitances and inductances and consequently, exhibit smaller effects. It is also noted that the two filters, although quite similar, suffer from substantially different discontinuity effects near the upper band. Nonetheless, the present simulation can successfully predict the filter performance with the discontinuities suitably modeled by lumped capacitances and inductances.

V. Illustrative Example of Chebyshev Filter Design

Once the stub sections and the junction discontinuities can be suitably analyzed, modeled, and simulated, the CPW bandpass filters can be successfully designed subject to the desired specifications. The design procedure can be better illustrated by a design example of the bandpass filter on a substrate of height 1.45 mm and dielectric constant $\epsilon_r = 4.2$. The feeding CPW is a 50 Ω line and has the dimensions of signal strip width 3.0 mm and slot width 0.34 mm, for which the effective dielectric constant is $\epsilon_{eff} = 2.25$. The desired filter specifications are

- pass band from 4–6 GHz
- ripple in the pass band 0.01 dB
- attenuation at least 20 dB at $f_1 = 2.4$ GHz.

The step-by-step design procedure is listed as follows.

1) The filter has the center frequency $f_o = 5$ GHz and fractional bandwidth $\Delta = 40\%$. The order N can be determined from the relations [10]

$$\begin{aligned} 0.01 &= 10 \log (1 + k^2) \\ 20 &\le 10 \log [1 + k^2 T_N^2(\widetilde{\omega}_1)] \\ &\cong 10 \log \{1 + k^2 \cosh^2 [N \cosh^{-1} (\widetilde{\omega}_1)]\} \end{aligned} \quad (12)$$

where $\widetilde{\omega}_1 \equiv (1/\Delta)|(f_1/f_o) - (f_o/f_1)|$ and $T_N(x)$ is the Nth order Chebyshev polynomial. For the present case, $k^2 = 0.0023$, $\widetilde{\omega}_1 = 4.0$, and the order should be at least $N = 3$. Hence, the filter should include four sections of open-end series stubs.

2) The low-pass prototype filter can be found by some simple equations [10, p. 597] from the given k^2 and N. The element values are $g_1 = g_4 = 0.629$ and $g_2 = g_3 = 0.970$.

3) By the design equations [12, p. 516], the values of the parameter $J \cdot Z_o$ are 1.000 for the first and fourth stub sections and 0.804 for the second and third stub sections.

4) The parameters $(Z_{avg}, K_{\Delta/2})$ of the coupled CPW's obtained by (10) are (100 Ω, 0.5) for the first and fourth sections and (82.3Ω, 0.488) for the second and third sections.

5) Now, it is desired to find the physical dimensions (s_1, d_1, s_2, d_2) of the coupled CPW's. By choosing a certain dimension fixed, say $s_2 = 3.0$ mm, the problem is reduced to the decision of the parameters (ξ, η, κ). For the first and fourth sections, the desired parameters are $Z_{avg} \cdot \sqrt{\epsilon_{eff}} = 150$ and $K_{\Delta/2} = 0.5$. Consulting the design chart Fig. 4(a) with fixed $\kappa = 0.3$ yields the parameters $\xi = 0.660$ and $\eta = 0.585$. However, the transmission lines analysis for the coupled CPW's with such dimensions yields the actual values of $Z_{avg} \cdot \sqrt{\epsilon_{eff}} = 147.5$ and $K_{\Delta/2} = 0.525$. The discrepancy can be compensated by consulting Fig. 4(a) again for the corrections $\Delta\xi$ and $\Delta\eta$ under a linear interpolation. The resultant parameters are $\xi = 0.646$ and $\eta = 0.696$. Similar approach can be employed for the second and third sections. The design chart Fig. 4(b) with $\kappa = 0.6$ is more appropriate for this case. The other two parameters are found to be $\xi = 0.740$ and $\eta = 0.839$.

6) The section length is close to a quarter wavelength at the center frequency, i.e., $l = v_o/(4f_o\sqrt{\epsilon_{eff}}) = 10$ mm. Trim off each stub section at both sides by a suitable amount, say 7%, to form the gaps. The lumped circuit models of the discontinuities is then calculated to

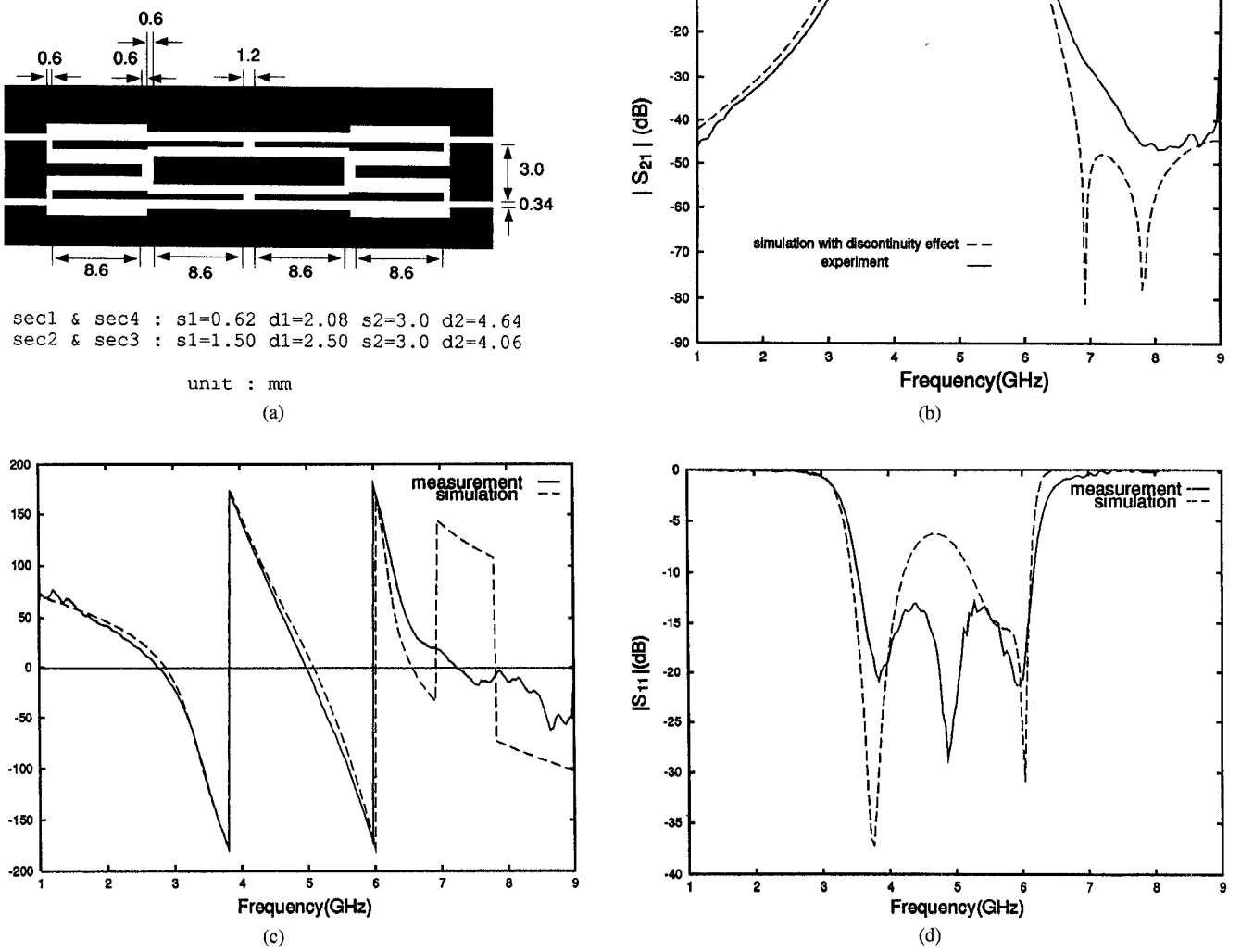

Fig. 9. Measurement and simulation results for a Chebyshev RBW filter. (a) Circuit layout, (b) magnitude of S_{21}, (c) phase of S_{21}, and (d) magnitude of S_{11}.

establish the complete circuit of the filter. The detailed frequency response can be simulated to inspect the filter performance.

7) Adjust the geometry dimensions, especially the section length and gap width, to compensate the discontinuity effects for optimal response. After several simulations, the section length of the coupled CPW's is chosen to be 9.8 mm. The signal strips in each section are trimmed by 0.6 mm at both sides to form the gaps.

The final circuit layout is shown in Fig. 9(a). The filter is fabricated and measured after a careful TRL calibration. Fig. 9(b) shows the simulation results and the measured data for the transmission coefficient $|S_{21}|$ of this filter. Fig. 9(c) shows the phase of S_{21}. The measured and simulation results are in good agreement and both justify that the filter response follows the specifications in the stop band. Fig. 9(d) shows the measurement and simulation results for the reflection coefficient $|S_{11}|$. It is found that the present design also provides reasonable filter performance in the pass band.

VI. Conclusion

This paper proposes a novel ribbon-of-brick-wall type coplanar waveguide bandpass filters which is compact in size and strictly uni-planar—requiring only one metallization plane and no air bridge. The design, analysis, simulation, and measurement techniques are presented for complete investigation of the RBW filter. The design originates from a new modeling of the open-end series stub in terms of asymmetrically coupled CPW's. Equivalence between the coupled CPW's and the admittance inverter is derived and drawn into some convenient design charts. By consulting the design charts, one can determine the geometric dimensions of all the stub sections to implement the desired admittance inverter and thus fulfill the bandpass filter design.

The discontinuities due to the stub junctions are modeled by lumped capacitances and inductances, which are calculated by employing efficient numerical techniques. A complete circuit consisting of coupled transmission lines models for the stub sections and lumped models for the junction discontinuities

is established to simulate the filter response. The simulation results can further aid in the adjustment of some dimensions, especially the section length and the gap width, to achieve a more successful design.

Some bandpass filter are fabricated to measure the scattering parameters. Good agreement between the measurement and simulation results validates the accuracy of the present modeling and analysis techniques. The measurement results also demonstrate that the proposed design procedure can successfully implement the RBW bandpass filter with satisfactory performance.

REFERENCES

[1] M. Houdart, "Coplanar lines: Application to broadband microwave integrated circuits," in *Proc. 6th Euro. Microwave Conf.,* Rome, 1976, pp. 49–53.

[2] N. I. Dib, L. P. B. Katehi, G. E. Ponchak, and R. N. Simons, "Theoretical and experimental characterization of coplanar waveguide discontinuities for filter applications," *IEEE Trans. Microwave Theory Tech.,* vol. 39, pp. 873–881, May 1991.

[3] A. K. Rayit and N. J. McEwan, "Coplanar waveguide filters," in *IEEE MTT-S Int. Microwave Symp. Dig.,* 1993, pp. 1317–1320.

[4] D. F. Williams and S. E. Schwarz, "Design and performance of coplanar waveguide band-pass filters," *IEEE Trans. Microwave Theory Tech.,* vol. MTT-31, pp. 558–566, July 1983.

[5] C. Nguyen, "Broadside-coupled coplanar waveguide and their end-coupled band-pass filter applications," *IEEE Trans. Microwave Theory Tech.,* vol. 40, pp. 2181–2189, Dec. 1992.

[6] C. Y. Chang, H. K. Chiou, T. H. Wang, and C. C. Chang "A CPW inductor coupled bandpass filter," in *Asia Pacific Microwave Conf.,* 1993, vol. 2, pp. 16.69–16.73.

[7] M. H. Mao, R. B. Wu, C. H. Chen, and C. H. Lin, "Characterization of coplanar waveguide open end capacitance—Theory and experiment," *IEEE Trans. Microwave Theory Tech.,* vol. 42, pp. 1016–1024, June 1994.

[8] C. Wei, R. F. Harrington, J. R. Mautz, and T. K. Sarkar, "Multiconductor transmission lines in multilayered dielectric media," *IEEE Trans. Microwave Theory Tech.,* vol. MTT-32, pp. 439–450, Apr. 1984.

[9] F. Romeo and M. Santomaro, "Time-domain simulation of n coupled transmission lines," *IEEE Trans. Microwave Theory Tech.,* vol. 35, pp. 131–136, Feb. 1987.

[10] R. E. Collin, *Foundations for Microwave Engineering,* 2nd ed. New York: McGraw Hill, 1992, ch. 8.

[11] G. L. Matthaei, L. Young, and E. M. T. Jones, *Microwave Filters, Impedance-Matching Network, and Coupling Structures.* Norwood, MA: Artech House, 1980, ch. 8.

[12] D. M. Pozar, *Microwave Engineering.* New York: Addison Wesley, 1990, ch. 9.

[13] C. W. Chiu and R. B. Wu, "A moment method analysis for coplanar waveguide discontinuity inductances," *IEEE Trans. Microwave Theory Tech.,* vol. 41, pp. 1511–1514, Sept. 1993.

[14] Hewlett-Packard Product Note 8510-8, "Network analysis: Applying the HP 8510B TRL calibration for noncoaxial measurements."

[15] M. Tran and C. Nguyen, "Wideband bandpass filters employing broadside-coupled microstrip lines for MIC and MMIC applications," *Microwave J.,* vol. 37, pp. 210–225, Apr. 1994.

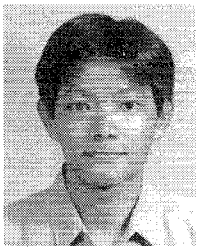

Fang-Lih Lin was born in Yunlin, Taiwan, Republic of China, in 1969. He received the B.S. degree in electronic engineering from National Chiao-Tung University, Hsin Chu, Taiwan, in 1992 and the M.S. degree in electrical engineering from National Taiwan University, Taipei, Taiwan, in 1994, where he is pursuing the Ph.D. degree in electrical engineering.

His research interest includes electromagnetic theory, analysis and design of microwave circuit.

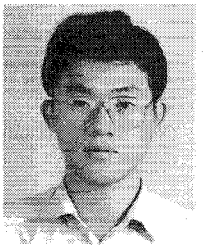

Chien-Wen Chiu was born in Maoli, Taiwan, Republic of China, in 1962. He received the B.S. degree from National Taiwan Normal University, Taipei, Taiwan in 1985 and the M.S. degree in electrical engineering from National Taiwan University, Taipei, Taiwan in 1990. Currently, he is pursuing the Ph.D. degree in electrical engineering at the National Taiwan University.

From 1990–1991, he was a Member of Computer & Communication Research Laboratory, where his primary work was on the research and development for Digital European Cordless Telephone. His research interest includes electromagnetic theory and transmission line discontinuities.

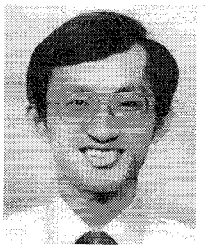

Ruey-Beei Wu (M'91) was born in Tainan, Taiwan, Republic of China, in 1957. He received the B.S.E.E. and Ph.D. degrees from National Taiwan University, Taipei, Taiwan, in 1979 and 1985, respectively.

In 1982, he joined the faculty of the Department of Electrical Engineering, National Taiwan University, where he is now a Professor. He was a visiting scholar at the IBM East Fishkill Facility, New York State, from March 1986–February 1987 and in the Electrical Engineering Department, University of California at Los Angeles, from August 1994–July 1995. His areas of interest include computational electromagnetics, dielectric waveguides, edge slot antennas, wave scattering of composite materials, transmission line discontinuities, and interconnection modeling for computer packaging.